Enhanced gravity wave activity in the mesosphere lower thermosphere region over Tirunelveli as a response to tropospheric convective event

K. Krishnapriya [a,b,*], S Sathishkumar [a], S. Sridharan [c]

[a] *Equatorial Geophysical Research Laboratory, Indian Institute of Geomagnetism, Tirunelveli 627 011, Tamil Nadu, India*
[b] *Manonmaniam Sundaranar University, Abishekapatti, Tirunelveli 627012, Tamil Nadu, India*
[c] *National Atmospheric Research Laboratory, Gadanki 517112, Pakala Mandal, Tirupati District, Andhra Pradesh, India*

Abstract

The recent upgrade of Medium-Frequency (MF) wind radar at Tirunelveli (8.7^oN, 77.8^oE) has improved the height and time resolution of the wind measurements, which are utilized in the present study to examine high frequency (in periods 20–60 min) gravity waves (GW) in the mesosphere and lower thermosphere (MLT) region. We observe, in addition to the dominant wave activity during equinox months, dominant episodes of high-frequency GW activities in the meridional winds during the times 31 May–4 June and 25–27 June 2019. Using the perturbation ellipse method, we infer the direction of propagation of the GW and it is found to be in the north–south plane. The GW activity in the MLT region exhibits anti-correlation with NOAA outgoing longwave radiation (OLR) and positive correlation with rainfall rates indicating the latent heat release due to tropical convection as the possible source of the GW. Besides, the presence of dynamical instability is inferred from the calculations using the radar wind and the spaceborne SABER (Sounding of Atmosphere using Broadband Emission Radiometry) temperature data suggesting a possible causality of convectively generated GWs dissipation.

© 2023 Published by Elsevier B.V. on behalf of COSPAR.

1. Introduction

Atmospheric gravity waves (GW) play a vital role in the dynamical coupling between different regions of the atmosphere and particularly in the energy budget of the mesosphere and lower thermosphere (MLT) (Hines, 1960). They are generated by a variety of mechanisms namely, topography, wind shear, jet streams, and frontal systems in the lower atmosphere. These GW can have periods ranging from minutes to hours, horizontal wavelength from several tens to thousands of kilometers, and vertical wavelength of several kilometers. They propagate upward with exponentially increasing amplitudes due to conservation of energy. However, under suitable conditions, they can become unstable and deposit their energy and momentum into the background flow in the upper atmosphere. Thereby, these waves contribute significantly to the circulation and thermal structure of the upper mesosphere and lower thermosphere region (Fritts and Alexander, 2003). Particularly, the GWs having high intrinsic frequencies and small horizontal scales are most effective at transporting momentum into the middle atmosphere (Fritts and

Vincent, 1987). There are many studies on GWs over mid-latitudes (Vincent and Fritts, 1987; Nakamura et al., 1996; Gavrilov et al., 1995; Manson et al., 1998; Jacobi et al., 2006). There are extensive studies on the climatology of GWs in the middle atmospheric parameters measured using different instruments which include Medium Frequency (MF) radars (Reid and Vincent, 1987), Middle and Upper Atmosphere (MU) radar (Tsuda et al., 1990), Mesosphere – Stratosphere – Troposphere radars (Fritts and Wang, 1991), Rayleigh Lidars (Senft and Gardner, 1991) and airglow imagers (Espy et al., 2004). Recently, Tian et al. (2020) studied the seasonal variation of high-frequency GW momentum fluxes using meteor radar observations from Langfang, China (39.4°N, 116.7°E) from 01 July 2010–31 July 2011. Their study reveals the high-frequency GW variance exhibits annual, semiannual and quasi 4 months oscillations.

Over tropics, the semiannual modulation of gravity wave activity with the range of 20 min–2 hr was reported in the MLT region using long term observations from 1993 to 2007 over Tirunelveli (Sridharan and Sathishkumar, 2008). Using MF radar observations from Pameungpeuk, Indonesia during 2004– 2010, Venkateswara Rao et al. 2012 reported correlations between short-period gravity-wave variances and the strength of semiannual oscillation (SAO) at the mesopause. Kovalam et al. (2011) reported the high-frequency GW with a range of 20 min–120 min using simultaneous wind observations from MF radars located at Tirunelveli and Pameungpeuk for the period February–March 2010 and provided the evidence of GW modulation in the tides and planetary waves. As the latent heat release in the deep tropical convection has been suggested as a potential source for the generation of gravity waves in the tropical latitudes, there are also studies, which have been attempting to relate the mesospheric GW variance with the tropical convection. Convection can generate a wide spectrum of GWs that have a large range of wavelengths, periods and amplitudes (Yue et al., 2013; Vadas et al., 2009). The vertical wavelength of the GWs generated by convection is about twice the depth of the heating (Holton et al., 2002). Usually, the thermal forcing by the latent heating is maximum in the mid-troposphere, and it is associated with convective storms that can generate high–frequency GWs. Dutta et al. (2009) studied the characteristics of high-frequency GW using MST radar and radiosonde observations of two deep convective days on 16 May and 5 June 2006 over Gadanki, they noticed an enhancement on convective days as compared to the normal days. Eswaraiah et al. (2018) studied the vertical coupling between the lower atmosphere and mesosphere through short period gravity waves using MST radar Rayleigh LIDAR measurements at Gadanki, India. They noticed the presence of short-period gravity wave with periods in the range 20 mins–2 hr in the troposphere and mesosphere during the deep convection days. GWs associated with thunderstorms, cyclones were also studied using radiosonde, MST radar, lidar, and airglow

imaging from the single–point measurements in the tropical region (Dhaka et al., 2002; Kumar, 2006; Das et al., 2012; Niranjan Kumar et al., 2011). Walterscheid and Christensen, (2016) studied the low latitude gravity wave variance in the mesosphere and lower thermosphere using SABER temperature observations and compared with the model simulation of wave generated by deep tropical convection. Their results reveal that large temperature deviations at mesospheric heights are found over geophysical regions where deep tropical convection is known to occur.

There are numerical simulation and theoretical studies on the excitation and effects of GWs and their role in providing a mean forcing on the middle atmosphere (Fovell et al., 1992; Alexander et al., 1996; Horinouchi et al., 2002; Kawashima, 2003). Miyoshi and Fujiwara, (2009) investigated gravity waves in the equatorial thermosphere and their relation to lower atmospheric variability using general circulation model results. Their study reveals the presence of short-period GW activity in the thermosphere and upward propagation from the lower atmosphere when the cumulus convection is enhanced. Most of the numerical simulations and observational studies reported that convectively generated short-period GWs in the tropical region play an important role in middle atmosphere global circulations changes (Fritts and Alexander, 2003). Some of the earlier model simulation studies show the vertical propagation of gravity waves from the troposphere to the thermosphere (Horinouchi et al., 2002; Miyoshi et al., 2014; Vadas and Fritts, 2004; Miyoshi and Fujiwara, 2008; Yiğit et al., 2008; Yiğit and Medvedev, 2010). For example, to study the vertical propagation of the sub-small scale gravity waves from the troposphere to the ionosphere, Yiğit et al. (2008) have implemented the extended parameterization into the Coupled Middle Atmosphere and Thermosphere-2 GCM (CMAT2) model, and simulated to have a global view of the small scale gravity wave propagation into the thermosphere. However, high-resolution data sets are required to study the characteristics, variabilities, and impacts of the high-frequency gravity waves. The scarcity of the high resolution data sets, the uncertainty remains in quantitatively estimating the effects of GWs due to the poor parameterization and representation in climate models.

GW information is scarce in the equatorial latitude due to observations limited to a few locations only. Over Tirunelveli, GW have been mainly carried out using an all–sky imager and MF radar. However, the imager observations are limited to cloud-free nights, which are sparse over tropical latitudes. Earlier, the sampling rate of MF radar was low. With the recent upgradation, the sampling rate is increased from 2 min to 1 min and there is an improvement in the data acceptance rate also. During May–June 2019, the data acceptance rate is relatively higher (shown in Fig. 1) and it has enabled us to examine high frequency (20–60 min) gravity waves and examine their relationship with the wave sources in the lower atmosphere.
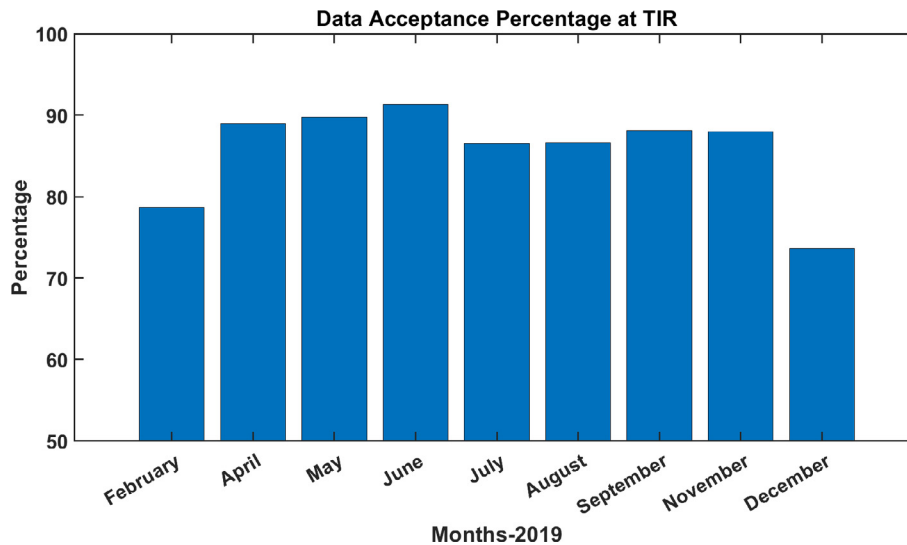
Fig. 1. Represents monthly data acceptance percentage at tirunelveli at 88 km during the month of February- December 2019.

This paper is organized as follows. The following section gives a brief introduction of the Medium Frequency (MF) radar, Reanalysis data sets, Thermosphere Ionosphere Mesosphere Energetics and Dynamics (TIMED) - Sounding of the Atmosphere using Broadband Emission Radiometry (SABER) temperature data, Tropical Rainfall Measuring Mission (TRMM) precipitation data, Outgoing Longwave Radiation (OLR). In section 3, a description of the methods we used to retrieve GW parameters is explained and the discussion of the GW enhanced events impacts in the MLT region. Concluding remarks can be found in section 4.

2. Data collection and analysis

2.1. Tirunelveli MF radar winds

The Medium Frequency (MF) radar located at Tirunelveli (8.7°N, 77.8°E) in the spaced antenna mode is operating at the frequency of 1.9 MHz provides zonal (u) and meridional (v) wind data in the altitude region 70–110 km with a resolution of 2 km and time resolution of 1 min. The radar beam is linearly polarized, as the station is near the dip equator. The MF radar system at Tirunelveli was upgraded in 2019 and receivers upgraded to 16 bit digitization. The operational height range of the radar has expanded up to 70–110 km, in particular, accuracy above 88 km improved considerably and one minute time resolution provide excellent dataset to study the MLT dynamics. In the present study, the wind data of May and June 2019 are utilized. Fig. 1 shows the data acceptance percentage at 88 km during February–December 2019 over Tirunelveli. Though the sample rate is 1 min, some data are rejected if they do not satisfy the data acceptance criteria (Briggs, 1984). Hence, the data for zonal and meridional wind components were averaged in 7 min sample bins. The 7 min averaged data are available with minimum data gaps as

shown in Fig. 1. Time series of 7 min samples of u and v were then plotted to find out the important wave components and 24 and 12 h tidal components present over Tirunelveli. 20–60 min GW components are then extracted by subtracting the other wave components from the data by applying the Butterworth filter. Finally GW variances in both the wind components ($\overline{u'^2}$, $\overline{v'^2}$) for the period of 20–60 min were computed from the data after application of Butterworth filter. It enables us to study the high frequency GW with the range of 20–60 min period in the MLT region. Morlet wavelets are used to find out the wave activity during May–June month over Tirunelveli other than GWs. The advantage of wavelet analysis over other time–frequency methods (such as the windowed Fourier transform) lies in the automatic scaling of the window along with the interrogating waveform, yielding optimal simultaneous detection of both high- and low- frequency signal components.

2.2. Reanalysis data sets

Precipitation data are used to identify the occurrence of deep tropical convection in the tropical region. We utilized the ERA5 reanalysis data which is a fifth-generation reanalysis produced by European Centre for Medium-range Weather forecasting ECMWF convective precipitation data provide high accuracy (one-hour resolution) to understand the local deep convection over the tropical region (Hersbach et al., 2020). Convective precipitation was plotted over 60° E– 95° E longitude and 0° N–25° N latitude which includes Tirunelveli (8.7°N, 77.8°E).

2.3. TIMED-SABER temperature data

The temperature profile in the stratosphere, mesosphere and lower thermosphere (SMLT) region is obtained from

the Sounding of the Atmosphere using Broadband Emission Radiometry (SABER) is a sensor on board the Thermosphere Ionosphere Mesosphere Energetics and Dynamics (TIMED) satellite that provides kinetic temperature and a few chemical compositions in the SMLT region. The satellite was launched in January of 2002 and it orbits at an altitude of 625 km with an inclination angle of 74.1°. The SABER scans the atmosphere from 10 km to 180 km in 58 s and can cover the latitude circle from winter hemisphere 53^0 to the summer hemisphere 83^0 (Liu et al., 2017; M.G. Mlynczak, 1997). SABER level-2A data present a vertical resolution of 400 m, adequate for studying GWs. We choose the SABER pass data between the latitude of 6° N and 10° N and the longitude of 75° E and 80° E.

2.4. TRMM precipitation data

The Tropical Rainfall Measuring Mission (TRMM) is a joint space mission between NASA and Japan's National Space Development Agency designed to monitor and study tropical and subtropical precipitation and the associated release of energy. This daily accumulated precipitation product is generated from the research-quality 3-hourly TRMM Multi-Satellite Precipitation Analysis TMPA (3B42). The result is given in mm. It has a spatial resolution of 0.25°latitude × 0.25°longitude. Daily TRMM rainfall data averaged between the latitude of 7° N–12° N and longitude of 75° E–80° E. TRMM data is used to produce composite picture of the life cycle of convection over Africa and the tropical Atlantic (Futyan and Del Genio, 2007). Data from the TRMM precipitation radar and Lightning Imager Sensor over the regions of Atlantic and Africa regions are allowing a composite picture of the system evolution to be built up.

2.5. Outgoing longwave radiation

The outgoing longwave radiation (OLR) data are obtained from the National Center for Environmental Prediction (NCEP) and they have been used as a proxy for convective activity. Low OLR values indicate the presence of deep convective clouds. The OLR data has a spatial coverage of 2.5°latitude × 2.5°longitude global grid (144x73). The daily OLR data at 8° N averaged for the longitudes 75.5° E–79.5° E are used to show the OLR variation near Tirunelveli. Kiladis et al. 2014 developed two univariate indices of the Madden–Julian Oscillation (MJO) based on outgoing longwave radiation to track the convective component of the MJO. They utilized the standard daily 2.5° resolution OLR dataset that has been interpolated in time and space to replace missing values (Liebmann and Smith, 1996).

3. Results and discussion

The monthly mean of GW variance in the meridional wind and zonal wind during February–December 2019 is depicted in Fig. 2. In the month of March, the MF radar is not functioning due to technical issues and there is no continuous data present in the month of October 2019. The monthly mean GW variance in the meridional component is presented except for these two months. As can be seen in the figure, an increase in wave activity with the variance of 140 m^2s^{-2} is noticed during the period June–September. The ratio of monthly mean variance of meridional and zonal components is greater than 1. Previous studies suggest that GW activity is more in the equinox (March–April and September–October) than in the solstice in the mesosphere region (Sridharan and Sathishkumar, 2008; Venkateswara Rao et al., 2012). However, we
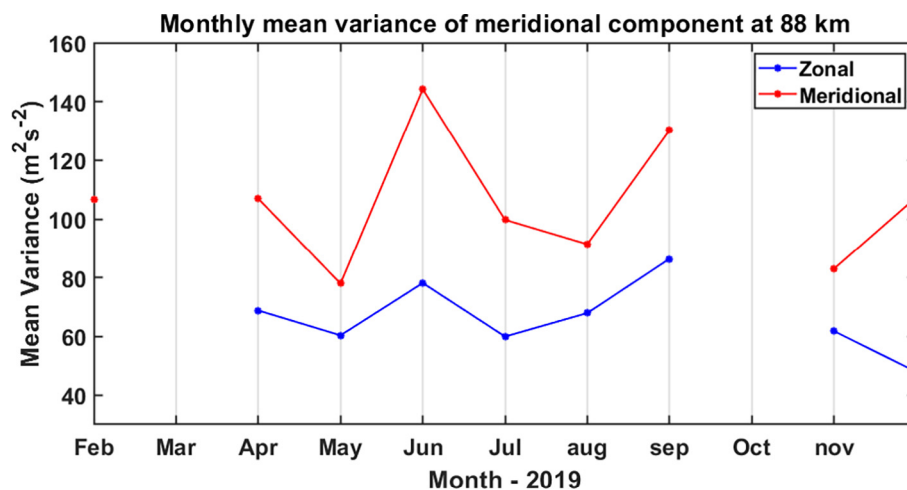

Fig. 2. Monthly mean of the variance of the meridional wind component and Zonal wind component in the 88 km height over Tirunelveli during February to December 2019.

observed an enhanced GW activity peak during June 2019 over Tirunelveli. We further investigate this enhanced GW activity, its possible source, and its influence on the MLT winds.

The presence of dominant wave periods can be inferred from the power spectrum of the wind components. The spectra of the zonal and meridional winds at 88 km derived from 7 min averaged wind data for the months May-June 2019 are presented in Fig. 3. The spectrum of zonal wind over Tirunelveli shows spectral peaks 24, 12 and 8 hr associated with the tidal components and spectral peaks near, ~ 6 – day and ~ 25 – day periods associated with planetary waves. The diurnal tide is the dominant component of both zonal and meridional winds. The meridional wind spectrum shows a broad peak around 2–3 days due to the presence of quasi-two day wave. The quasi two-day wave is a strong feature of low latitude (Gurubaran et al., 2001). The winds averaged for 7 min at heights from 86 to 92 km are subjected to harmonic analysis to remove the dominant tidal component of 24 hr and 12 hr components which were subtracted from the data. The Butterworth filter is applied to select 20–60 min period frequency of GWs from the residual wind data and then the daily variance is estimated to study the behavior of the high-frequency GWs in the MLT region.

The daily zonal (red) and meridional (blue) wind variances for the period of May and June 2019 are plotted in Fig. 4 for the altitudes 86, 88, and 90 km over Tirunelveli. As can be seen in the figure the GW variance in both merid-

ional and zonal components exhibits considerable day-to-day variability. Moreover, the GW variance in the meridional wind is found to be much larger than that in the zonal component. During the first week of June, the wind variance in the meridional wind is relatively larger of about ~ 700 m^{2}s^{-2} than the other days in the month of June in all heights over Tirunelveli. Though there is another maximum variance of ~ 500 m^{2}s^{-2} noticed at the end of June 2019, it is weaker than the maximum observed during the first week of June. These results can be compared with the previous result of GW observational studies made at equatorial sites. Vincent and Lesicar, (1991) found daily values of variances in the range 50–200 m^{2}s^{-2} for GWs in 4 min–1 hr at 86 km altitude in MF radar measured winds over Christmas Island. The studies on GWs of 20 min–4 hr band made at Hawaii in the altitude region between 86 and 92 km (Connor and Avery, 1996; Gavrilov et al., 2004) have also reported values in the range of 200–400 m^{2}s^{-2}. Another GW study at equatorial site Trivandrum, from meteor radar data (Antonita et al., 2008) reported total mean square amplitudes in the range of 300–400 m^{2}s^{-2} between 86 and 92 km. At Tirunelveli, the GW variance increases when the height increases from 86 to 90 km. Kovalam et al. (2011) reported an enhancement in the GW variance in meridional wind during February and March 2010 over Tirunelveli. They noticed a peak during the equinox period which clearly indicates the seasonal pattern of GW activity over Tirunelveli (Sridharan and Sathishkumar, 2008). This
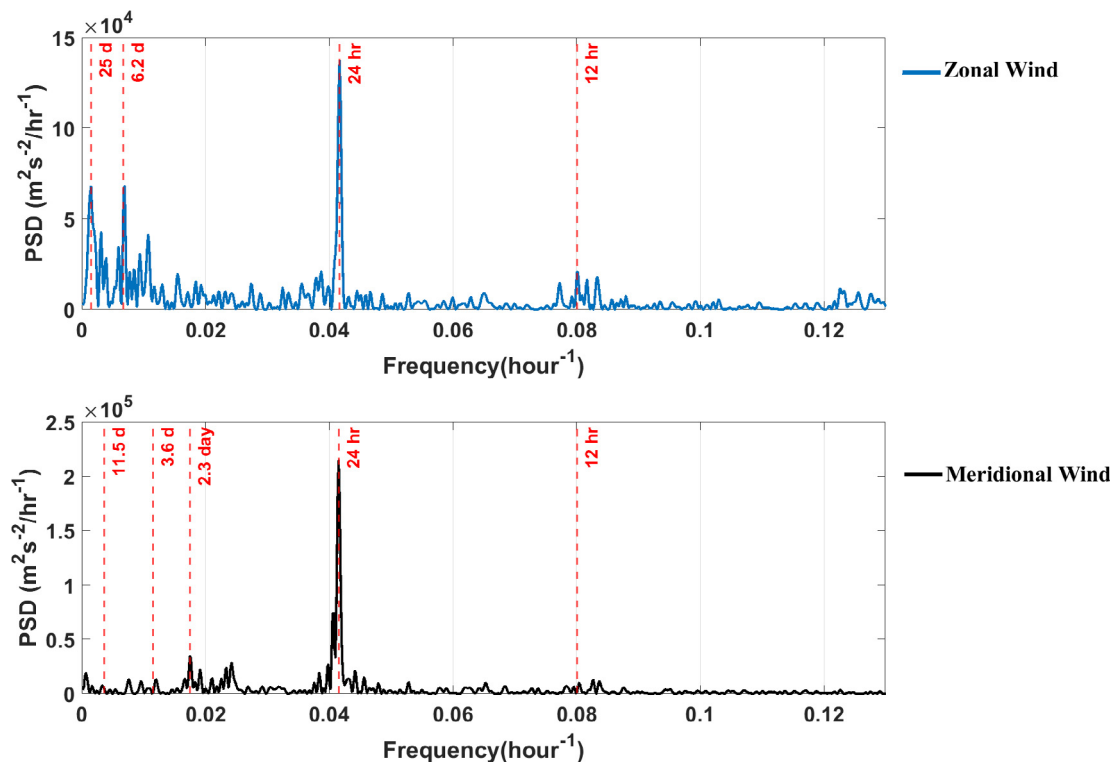

Fig. 3. Frequency spectrum of 7 min averaged zonal (top) and meridional wind (bottom) at 88 km during May and June 2019 over Tirunelveli.
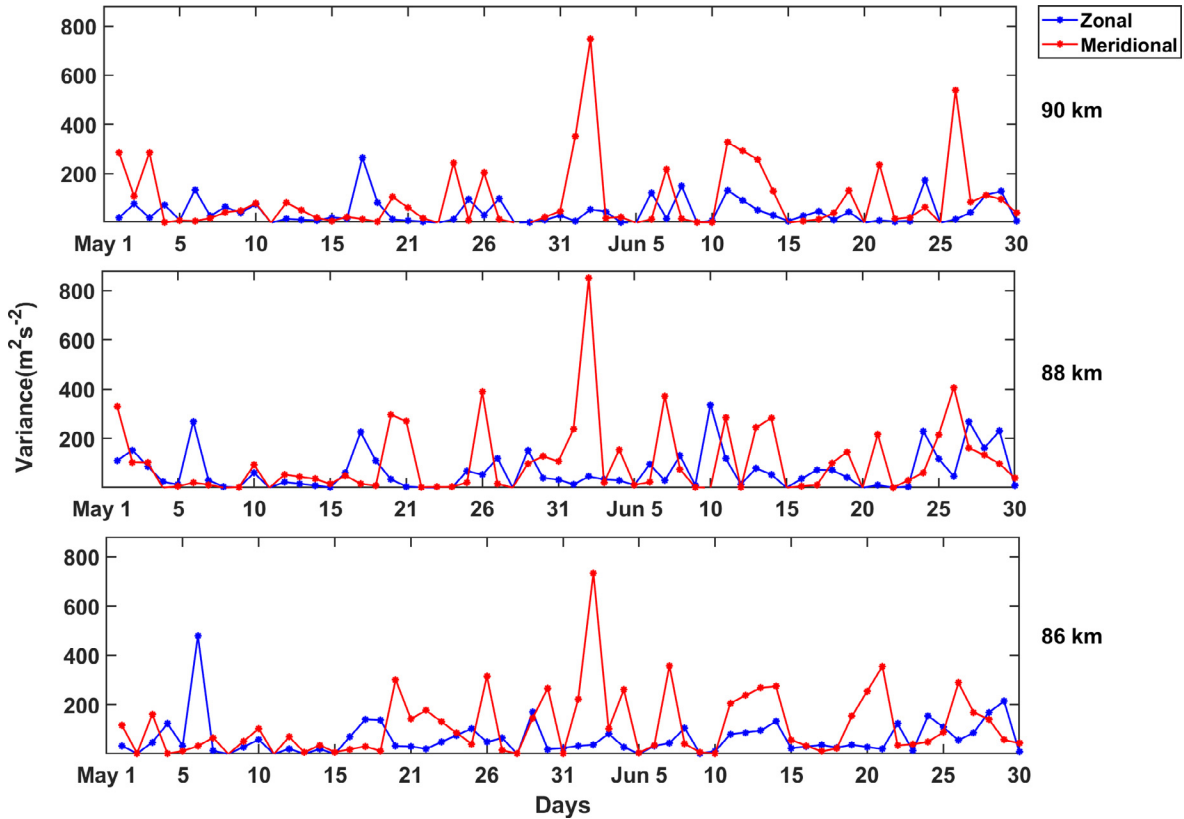
Fig. 4. Daily variations of (blue) zonal and (red) meridional GW variance (20–60 min) during May-June 2019 for the altitudes 86, 88, and 90 km over Tirunelveli.

preferential enhancement of GWs variances in meridional wind has also been noted in the earlier MF radar wind observations (Vincent et al., 1987; Isler and Fritts, 1996). In the present study, the GW variance in the meridional wind also shows a strong large variability with 2–4 days (Fig. 3). It may be due to the GW interaction with the planetary waves particularly the quasi-2-day wave. Fig. 5 compares the zonal and meridional wind variances between three years 2019, 20 and 21. It is very clear from the figure that the GW activity in the year 2019 is peculiarly stronger, when compared to the other years 2020 and 2021. GW variance is considerably less in 2020 and 2021.

The large difference in the variance between zonal and meridional components reveals the anisotropy in the horizontal propagation of GW activity in the MLT region. The anisotropy in the wave propagation direction is noted due to strong contribution from meridionally propagating waves. These observations suggest that the wave field is partially polarized and wave motions aligned more in the north–south direction than in the east–west direction.

Sridharan and Sathishkumar, (2008) found the direction of wave motions in NW/SE quadrant by using the MF radar winds data. To investigate the direction of propagation of GW activity in the MLT region, we adopt a perturbation ellipses which provides the propagation direction of the wave. The perturbation of wind velocity $\xi\prime$ is connected with perturbations of zonal u' and meridional v' wind components as follows

$$\xi' = u'sin\varphi + v'cos\varphi \tag{1}$$

With ϕ being the clockwise direction from the North. The total variance $\overline{\xi'^2}$ in the direction of ϕ

$$\overline{\xi'^2} = \overline{u'^2} \sin^2 \phi + \overline{v'^2} \cos^2 \phi + r\sqrt{\overline{u'^2 v'^2}} \sin 2\phi \tag{2}$$

with r as the correlation coefficient between u' and v'. The above equation describes an ellipse with the direction of the main axis as the preferred propagation direction.

Fig. 6 represents the perturbation ellipses for individual days in the month of June 2019 obtained for two heights intervals of 86 and 88 km over Tirunelveli. In general, the propagation direction is in the northwest-southeast direction. However, when there is an enhancement of gravity wave activity on days 2 June and 26 June 2019, the gravity wave propagation direction is in the North-South plane. It is important to mention here that the actual direction of wave propagation was not computed as we have not used the vertical velocity data in this work. Although the actual direction of wave propagation is unknown, it is apparent that the horizontal distribution has a strong meridional bias. An earlier report from the Indian subcontinent by Narayanan and Gurubaran, 2013 also revealed northward propagation of GW for the year 2007 by using all sky imaging observations over Tirunelveli (8.7° N).

In general, latent heat release due to tropical convection is one of the important sources for the generation of high
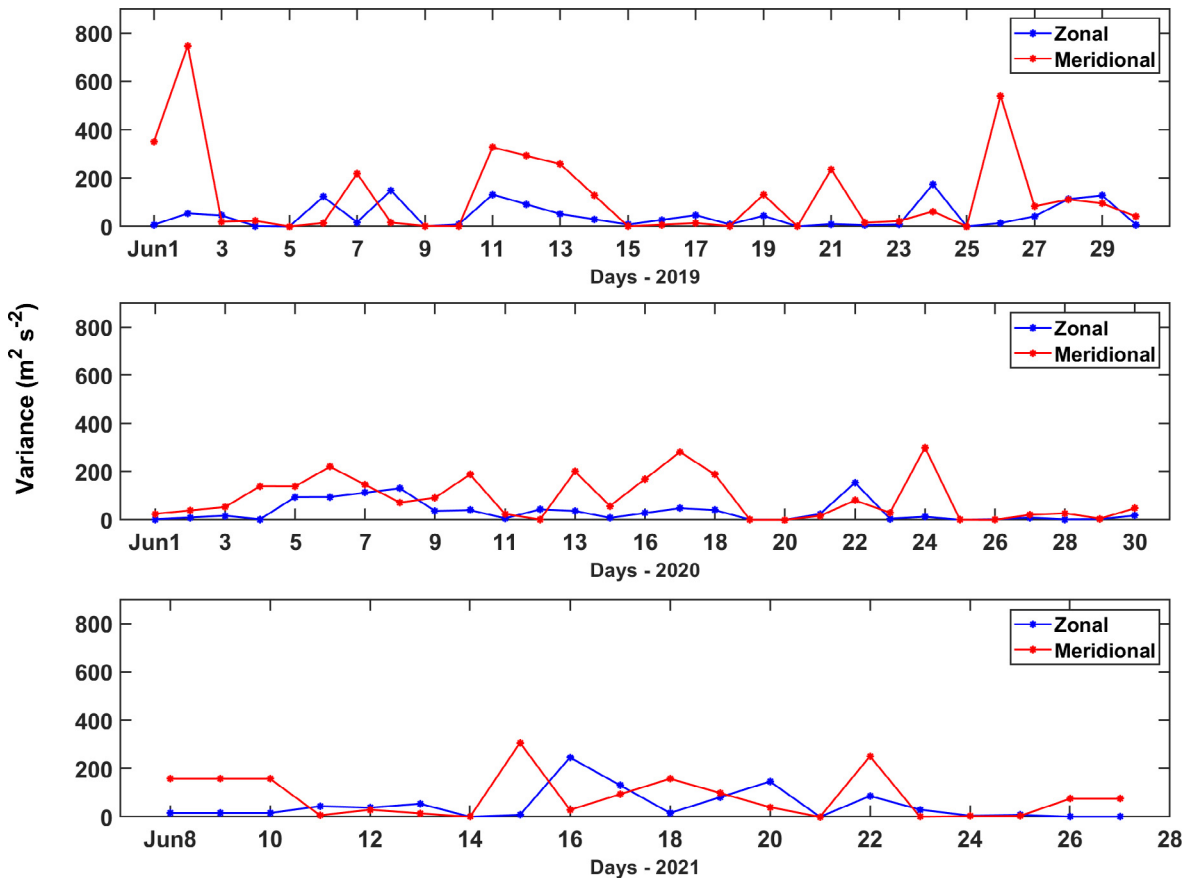
Fig. 5. Daily variations of (blue) zonal and (red) meridional GW variance (20–60 min) at Tirunelveli during 2019, 2020 and 2021 at an altitude of 90 km.
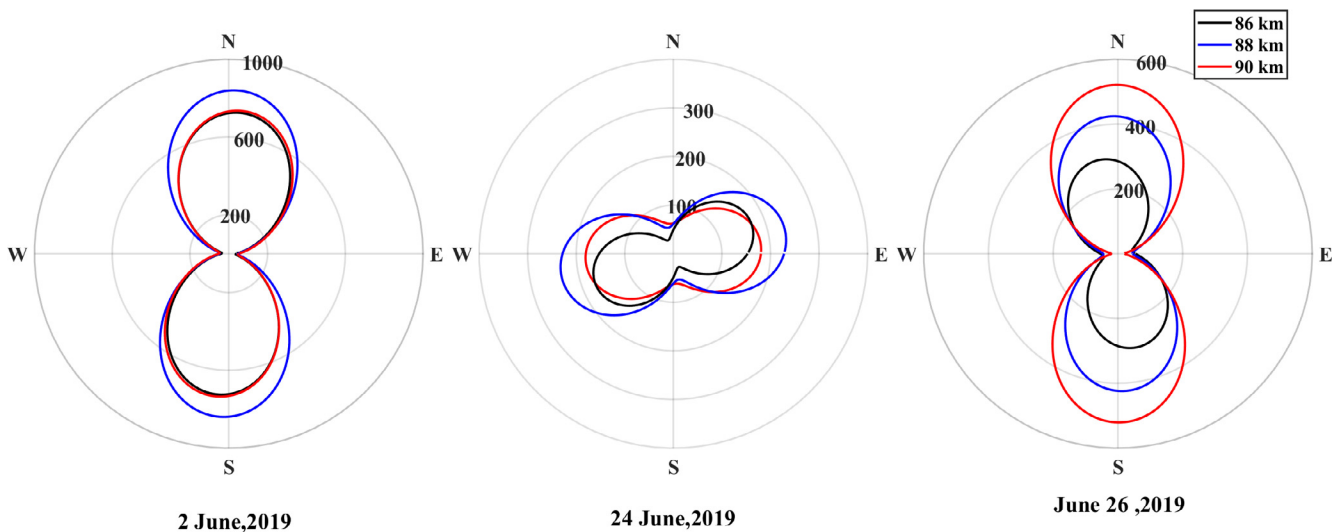

Fig. 6. Polar plot of dominant directions of horizontal Propagation over Tirunelveli at different intervals between heights 86–90 km on convective days.

frequency gravity waves in the atmosphere. Yue et al. (2014) reported on the first simultaneous space-borne observations of concentric GW patterns in the stratosphere and mesosphere over the Indian Ocean excited by Tropical Cyclone Mahasen. It is investigated whether the enhance-

ment of the GW variance in the meridional wind during June observed in the present study is due to tropical convection. In order to study the link between GW enhancement and tropical convection, the convective precipitation dataset from the ERA5 reanalysis is used.
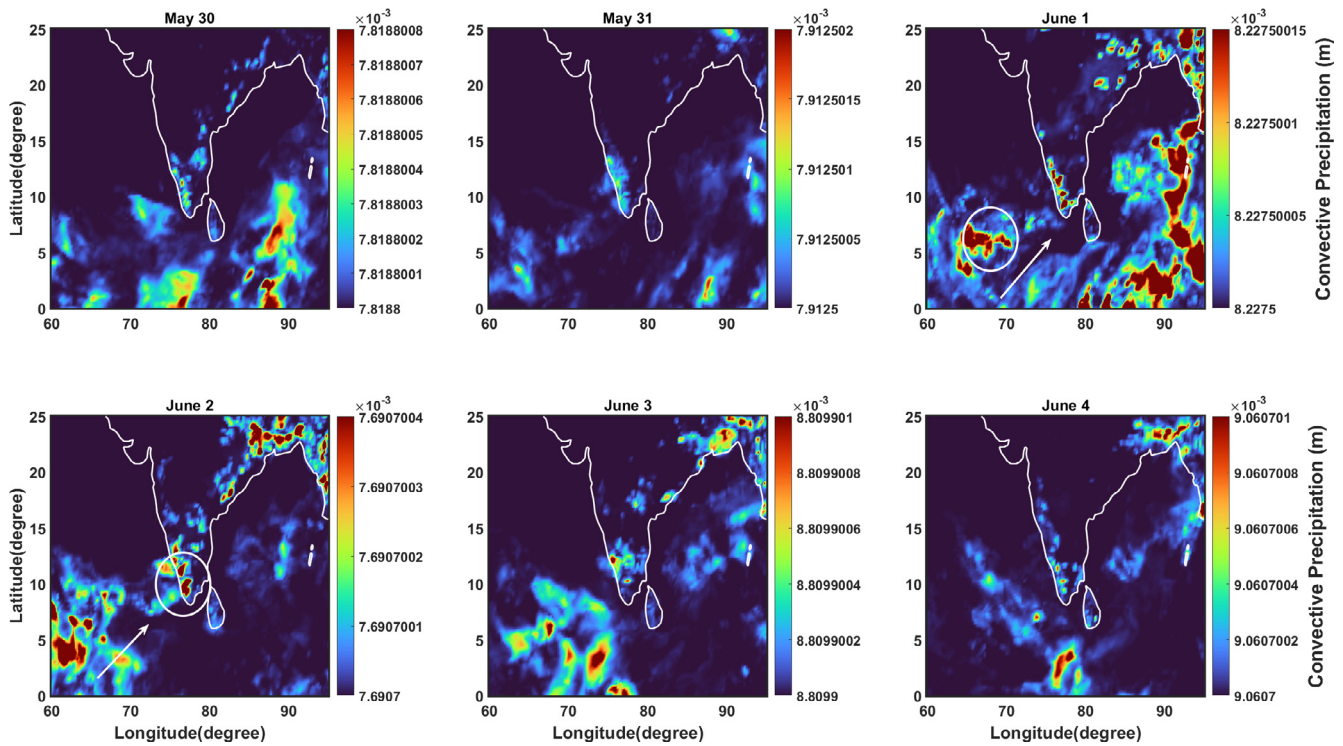
Fig. 7. Daily Convective Precipitation (mm) over Tirunelveli from May 30 – June 4, 2019.

There are two prominent enhancements in the GW activity in the meridional wind at 88 km over Tirunelveli; one during the first week and the other during the last week of June 2019. Hence, we choose six days of daily precipitation movement for the periods 30 May–04 June 2019 and 22–27 June 2019 to study the link between convection and GW activity in the MLT region.

Fig. 7 shows the longitude-latitude cross-section of daily convective precipitation motion from ERA5 during 30 May – 04 June 2019. As can be seen in Fig. 7, the convection is initiated near longitudes 60° E–75° E on May 31 and then reached close to Tirunelveli on 2nd June with an intensity of about 7 mm/day. The precipitation marked by a circle on June 1 is spread into the region 75° E–85° E and 5° N–15° N and the intensity of the precipitation diminishes when it reaches the land area. On 2nd June, the convective precipitation attained maximum close to Tirunelveli and it clearly matches with the enhancement of GW variance in the meridional wind in the MLT region over Tirunelveli. After, 3rd June, the circled convective motion is moved into the north eastern region of India.

Fig. 8 is similar to Fig. 7, but for the period 22–27 June 2019. Convective precipitation is highlighted by a circle in figure. From the figure, we can infer that the precipitation motion is noticed at about 65° E–75° E on 22nd June (Arabian Sea) and it appears to move towards the western part of India on 24th June, further extends on day 25 and later spread to the southern part of India on 26th June 2019. Traces of the precipitation spreads along the Arabian Sea

(marked by an arrow in figure) to the southern part of India with an intensity around 7–8 mm/day. The precipitation motion and horizontal direction of the GW (Fig. 6) over Tirunelveli are consistent with each other. It suggests that convectively generated gravity waves in the lower atmosphere may be the source of the GW enhancement in the MLT region over Tirunelveli.

The connection among the background meridional winds, GW daily variance, and rainfall rate is shown in Fig. 9. The left top panel in the figure represents the time-altitude cross-section of daily mean meridional winds over Tirunelveli for the period of 01 May–30 June 2019. As the mean meridional winds at MLT heights are largely driven by GWs, it is investigated whether there is any noticeable change in the winds. As expected, the daily mean meridional wind is observed to be largely strong equatorward with a magnitude of about $\sim 30 \text{ ms}^{-1}$ during 2–4 June and 25–27 June 2019 over Tirunelveli. While these time series reveal considerable variability, the daily meridional wind is stronger when the GW variance reaches a peak over Tirunelveli. The wavelet spectrum of meridional winds clearly show the quasi two-day wave during 25–28 June over Tirunelveli. In response to the quasi-two-day wave the GW variances are modulated well over Tirunelveli from the mid of the June onwards. The 2-day modulation of GW variance was observed by Isler and Fritts, (1996) and Herman et al. (1999). In Fig. 9, right bottom figure represents the time-latitude cross-section of daily rainfall precipitation taken from TRMM averaged over the
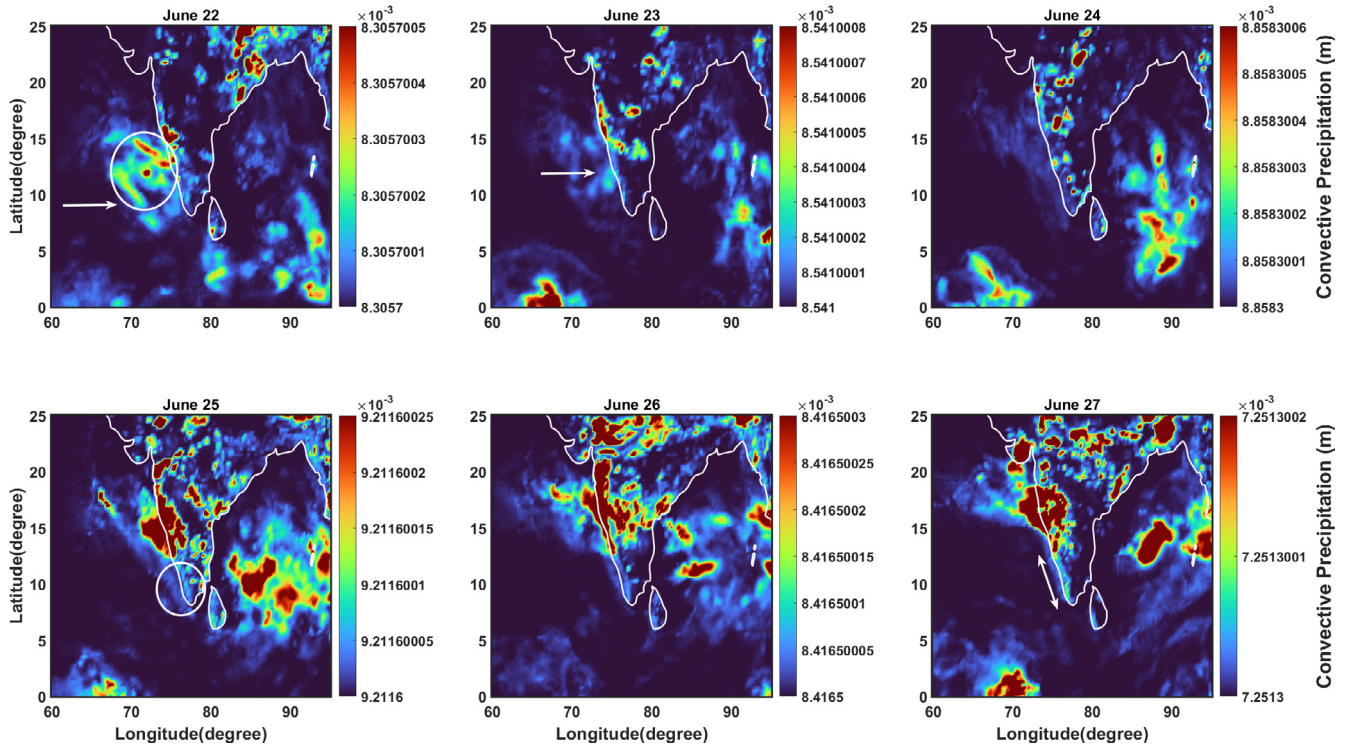
Fig. 8. Daily Convective Precipitation (mm) over Tirunelveli from June 22 – June 27, 2019.
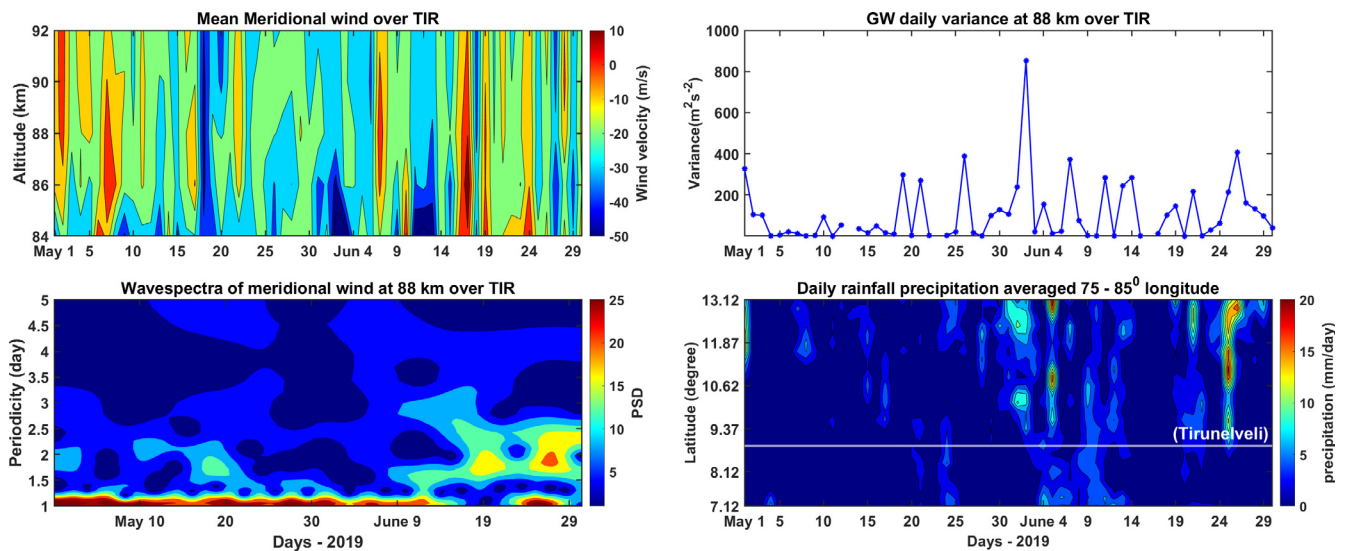

Fig. 9. Mean meridional wind, GW daily variance, Wave spectra of meridional wind and rainfall rate from TRMM over Tirunelveli during May – June 2019.

longitude cross-section of 75° E–85° E. During the high GW variance days the rainfall precipitation was about 10–20 mm/day over Tirunelveli.

To examine the convective activity during June 2019 in detail, we utilized outgoing longwave radiation (OLR) as a proxy for convection in the tropical region. The daily OLR averaged at 75.5° E–79.5° E for the month of May and June 2019 along with GW variance in the meridional wind at 88 km over Tirunelveli is presented in Fig. 10.

The OLR color bar is reversed in order to relate to the convection, as low OLR is a proxy for the convection. It is interesting to observe that the low OLR values are different for each month. During May, the OLR values are high of $\sim$ 240–260 Wm^{-2} and they are low during June ($\sim$180–190 Wm^{-2}). On the first week of June OLR is $\sim$ 180–200 Wm^{-2} and the GW variance is $\sim$ 700 m^{2}s^{-2}. During the last week of the June, the OLR is $\sim$ 200 Wm^{-2} and GW variance is 500 m^{2}s^{-2}. Very strong
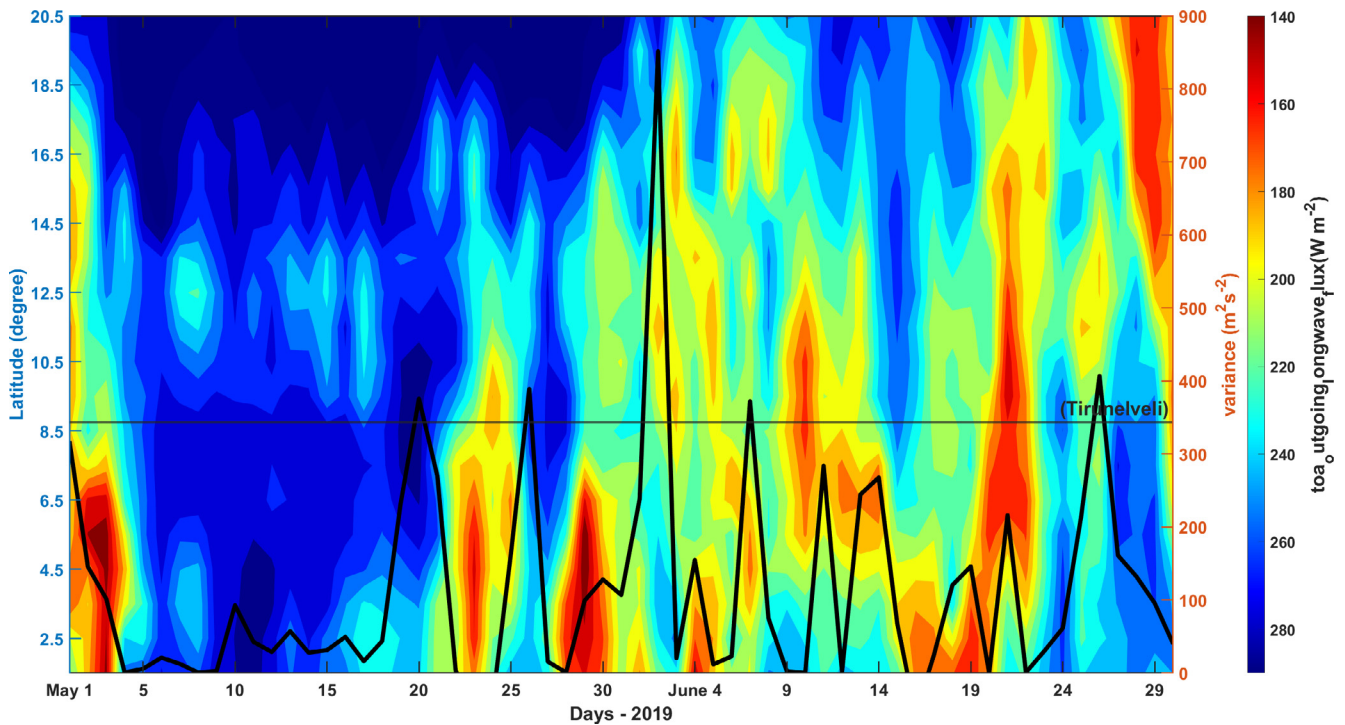
Fig. 10. OLR data for longitude sector 75.5° E– 79.5° E and for different latitudes from 1.5° N − 20.5° N during May-June contour plot. Daily values of wave variance of June month smoothed and overlaid.
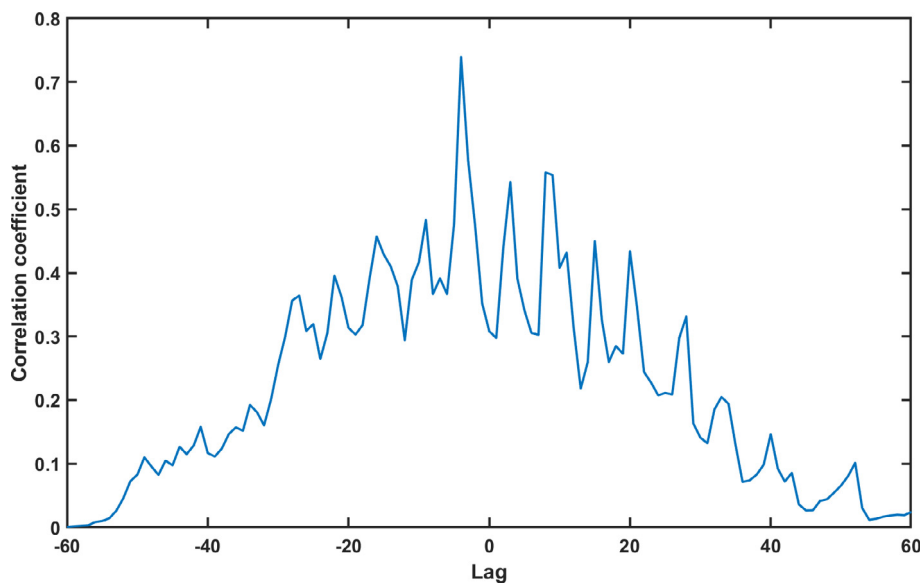

Fig. 11. Correlation between the GW variance and convective precipitation during May-June 2019.

correlation exists between the latent heating OLR over the tropics. Low OLR is linked to amplified heating in the tropics, tied to latent heat release (Zhang et al., 2017). These results suggests the presence of latent heat release around these days and the enhancement of GW variance in the MLT region may be generated due to deep tropical convection over Tirunelveli. Fig. 11 shows the correlation between the GW variance and convective precipitation during May-June 2019. The correlation coefficient between

GW variance and precipitation is 0.73. The correlation is found to be decreasing while moving away from Tirunelveli.

Gravity waves transport heat, horizontal momentum, and constituents both vertically and horizontally and create an impact on the middle atmosphere dynamics. Studies have shown that gravity wave instability mechanisms include a combination of convective and dynamic properties (Sonmor and Klaassen, 1997). Instability processes
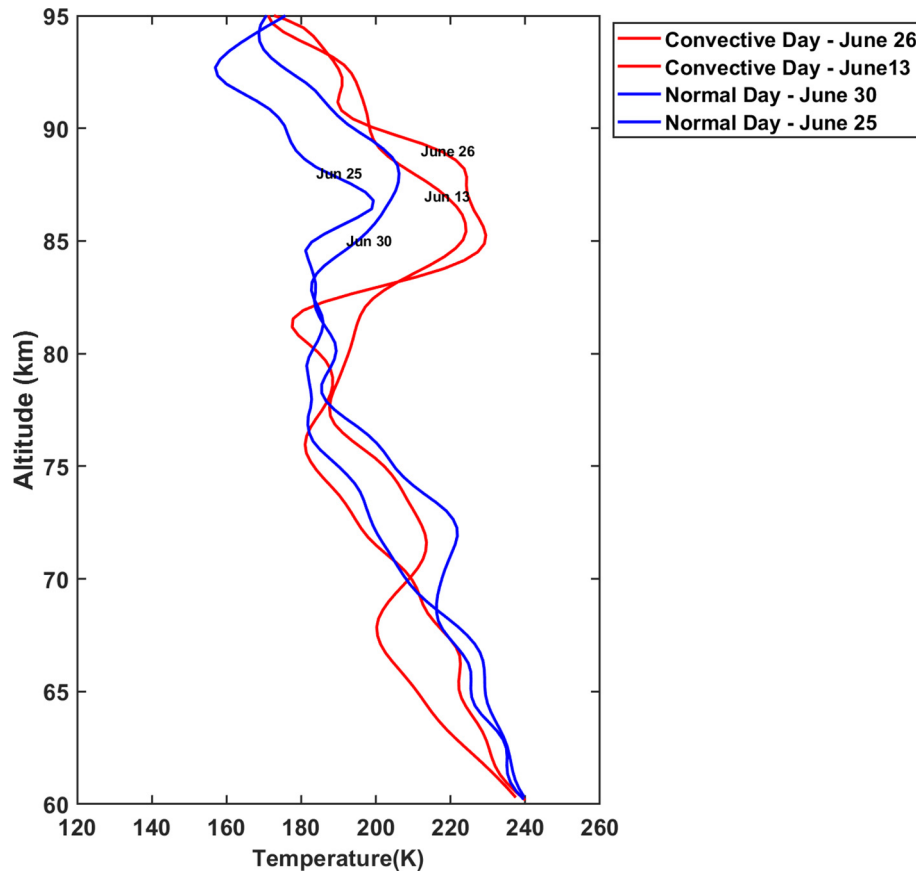
Fig. 12. SABER temperature vs altitude plotted for June 13, June 25, June 26, and June 30.

are believed to be responsible for altering the characteristics of gravity waves near the mesopause region. In order to study the stability properties and the presence of gravity waves requires height variation of both wind and temperature data. The propagation of gravity waves affects the background atmospheric parameters. In the present study, we use the height profile temperature data from the SABER instrument onboard TIMED satellite. To understand the temperature perturbation due to GWs, we further looked into the SABER temperature profiles during the deep convection days. Fig. 12 depicts the temperature profile of the convective days June 13 and June 26, normal days (low variance) June 30 and June 25. The SABER passage on June 26 was over 6.11° N, 80.73° E. As it was over 7.12° N, 76.89° E and also over 10.54° N, 77.49° E on June 13, the temperature profiles over these two locations are averaged and plotted. It reveals the signature of the GWs in temperature perturbations around 83–100 km. During the convective day, the temperature is enhanced by 26–47 K from the normal day profile. Negative gradient in temperature exists within 88–91 km. The steep negative temperature gradient makes the ambient atmosphere convectively unstable whereas, the shear in the horizontal velocity can trigger dynamical instability. The energetics in the upper mesosphere is mainly influenced by the pas-

sage of gravity waves that have larger spectral powers and are mainly responsible for altering mesospheric temperature. This indicates the presence of the GWs in the MLT region and the strong vertical coupling during the convection. Our results are consistent with earlier observations using sodium airglow photometer over Gadanki and Mt. Abu (Sarkhel et al., 2012).

Hodges (1969) and Lindzen (1981) suggested that the convective instability plays a significant role in the alteration of characteristics of GWs. Convective instability results whenever the environmental adiabatic lapse rate is greater than dry adiabatic lapse rate. This can be studied using the Brunt–Vaisala frequency (N).This is the frequency at which an air parcel oscillates when displaced vertically within a stable environment under the influence of buoyancy as a restoring force. The expression for N^2 is;

$$N^2 = \frac{g}{T_{(z)}}\left[\Gamma + \frac{dT(z)}{dZ}\right] \tag{3}$$

Where $\Gamma = \frac{g}{C_p}$ the adiabatic lapse rate.

$T_{(z)}$ neutral temperature at the height z; g is the acceleration due to gravity; C_p is the specific heat capacity at constant pressure and Γ is. Convective instability is implied by the negative values of the square of the buoyancy frequency N^2. Dynamical instability is also responsible for
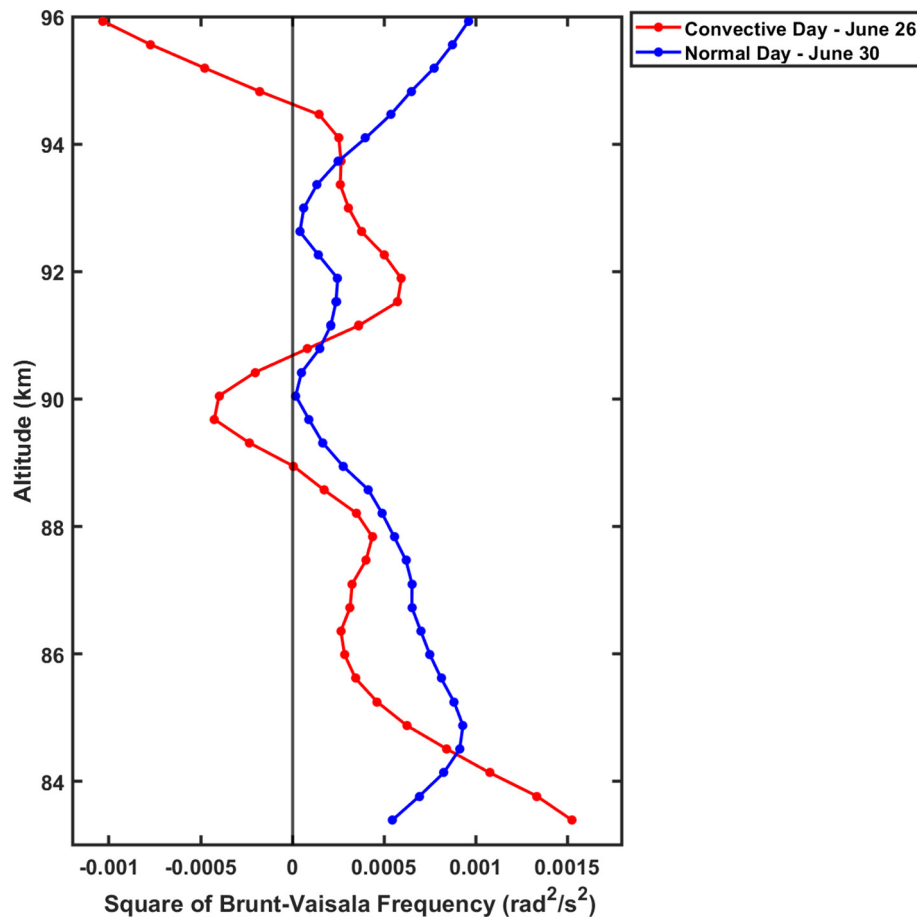
Fig. 13. Square of buoyancy frequency vs altitude plotted for June 26, and June 30.

altering the characteristics of gravity waves. The dynamical instability can be quantified using the dimensionless Richardson number. The expression for R_i is;

$$R_i(z) = \frac{N^2_{(Z)}}{\left(\frac{du}{dz}\right)^2 + \left(\frac{dv}{dz}\right)^2} \qquad (4)$$

Where $u(z)$ and $v(z)$ are the zonal and meridional winds (in m/s), respectively, at an altitude z. If $R_i < 0$, condition for convective instability and if $0 \leq R_i \leq 0.25$, condition for dynamical instability. Convective and dynamical instabilities occur in the mesosphere depending on critical values of N^2 and R_i.

Fig. 13 shows the altitude profile of square of the buoyancy frequency (N^2). Changes in background conditions do occur at the mesospheric heights because of the deposition of energy and momentum by the dynamics process (Narayanan et al., 2010). The value of buoyancy frequency is expected to be greater than zero for the upward propagation of the GWs in the atmosphere. Here at the height region 88–91 km the square of buoyancy frequency is negative indicating the unstable region of the mesosphere. At 89 km the value of N^2 is -2.3×10^{-4} s^{-2} and at 90 km it is -4.25×10^{-4} s^{-2}. At heights 89–91 km, the atmosphere is found to be convectively unstable. To test whether any

strong shears in the mesosphere, which can lead to dynamic instabilities, we examined the non-dimensional Richardson number for the height between 86 and 90, which is an indicator of dynamic instability. At 86 and 88 km, the Richardson number was 6.9645×10^{-5} and 7.0914×10^{-5} respectively. It is noticed that the Richardson number is in the range of 0–0.25 at 86 and 88 km indicating the dynamics instability. However, the Richardson number is -4.9127×10^{-5} at 90 km indicating the presence of convective instability.

4. Summary

In this work, an enhanced gravity wave activity observed in MLT meridional winds over Tirunelveli during 01 May–30 June 2019 is examined. Its variability; its possible source and its influence on the MLT winds are investigated.

Apart from the seasonal GW activity during the equinox months, an unusual enhancement over June month is observed. The GW having period, (20–60 min) variance in the meridional wind at 88 km noticed a peak of ∼ 800 (m/s)^2 in the beginning of June and a secondary peak at about ∼ 500 (m/s)^2 in the end of June 2019 as compared to other days over Tirunelveli. 2019 is peculiarly stronger,

when compared to the other years 2020 and 2021. The angular distribution of the GW shows that the plane of GW propagation is aligned in the NS direction. We have examined the GW activity in the month of June in terms of convection as the primary source for wave generation in the tropical region. The presence of tropical convection is observed when the peak GW variance is observed in the meridional component over Tirunelveli. The convective precipitation moves close to the Tirunelveli on the day GW variance reaches the peak and the convective precipitation motion direction is in good agreement with the direction of GW horizontal propagation. Our results indicate a strong anticorrelation between OLR and GW variance. Low OLR values associate with peak TRMM rainfall rates confirm the presence of tropical convection in causing the GWs variability in the equatorial MLT region. From daily mean meridional wind is noticed an intense equatorward wind when the GW reaches its peak in the month of June 2019. Changes in the background atmospheric parameters during the high GW variance indicate the vertical coupling of the atmospheric layers through the waves. The results presented here are from a case study in which the deep tropical convection is related to the occurrence of enhanced GW activity in the low latitude MLT region. Analysis of long-term observations and model results will provide a more complete understanding of the role of tropical convection on the MLT gravity wave activity and its influence on the circulation and this will be taken up in our future studies.

Declaration of Competing Interest

The authors declare that they have no known competing financial interests or personal relationships that could have appeared to influence the work reported in this paper.

Acknowledgements

References.

Alexander, M.J., 1996. A simulated spectrum of convectively generated gravity waves: propagation from the tropopause to the mesopause and effects on the middle atmosphere. J. Geophys. Res. 101 (D1), 1571–1588. https://doi.org/10.1029/95JD02046.

Antonita, T.M., Ramkumar, G., Kumar, K.K., Deepa, V., 2008. Meteor wind radar observations of gravity wave momentum fluxes and their forcing toward the Mesospheric Semiannual Oscillation. J. Geophys. Res. 113, D10115. https://doi.org/10.1029/2007JD009089.

Briggs, B.H., 1984. The analysis of spaced sensor records by correlation techniques. Int. Council Scient. Unions Middle Atmos. Program 13, 166–186.

Connor, L.N., Avery, S.K., 1996. A three-year gravity wave climatology of the mesosphere and lower thermosphere over Kauai. J. Geophys. Res. 101 (D2), 4065–4077. https://doi.org/10.1029/95JD03065.

Das, S.S., Uma, K.N., Das, S.K., 2012.MST radar observations of short-period gravity wave during overhead tropical cyclone. Radio Science. 47(02), 1-10.https://doi.org/10.1029/2011RS004840.

Dhaka, S. K., Choudhary, R. K., Malik, S., Shibagaki, Y., Yamanaka, M. D., and Fukao, S., 2002. Observable signatures of a convectively generated wave field over the tropics using Indian MST radar at Gadanki (13.5°N, 79.2°E).Geophys. Res. Lett., 29, 1872.https://doi.org/10.1029/2002GL014745.

Dutta, G., Ajay Kumar, M.C., Vinay Kumar, P., VenkatRatnam, M., Chandrashekar, M., Shibagaki, Y., Salauddin, M., Basha, H.A., 2009. Characteristics of high-frequency gravity waves generated by tropical deep convection. Case studies. J. Geophys. Res. 114, D18109. https://doi.org/10.1029/2008JD011332.

Espy, P.J., Jones, G.O.L., Swenson, G.R., Tang, J., Taylor, M.J., 2004. Seasonal variations of the gravity wave momentum flux in the Antarctic mesosphere and lower thermosphere. J. Geophys. Res. 109, D23109. https://doi.org/10.1029/2003JD004446.

Eswaraiah, S., Chalapathi, G.V., Kumar, K.N., Ratnam, M.V., Kim, Y. H., Prasanth, P.V., Lee, J., Rao, S.V.B., 2018. A case study of convectively generated gravity waves coupling of the lower atmosphere and mesosphere-lower thermosphere (MLT) over the tropical region: an observational evidence. J. Atmos. Sol.-Terres. Phys. 169, 45–51. https://doi.org/10.1016/j.jastp.2018.01.005.

Fovell, R., Durran, D., Holton, J. R., 1992. Numerical Simulations of Convectively Generated Stratospheric Gravity Waves, Journal of Atmospheric Sciences. 49(16), 1427-1442.https://doi.org/10.1175/1520-0469(1992)049<1427:NSOCGS>2.0.CO;2

Fritts, D.C., Alexander, M.J., 2003. Gravity wave dynamics and effects in the middle atmosphere. Rev. Geophys. 41, 1003. https://doi.org/10.1029/2001RG000106.

Fritts, D.C., Vincent, R.A., 1987. Mesospheric momentum flux studies at Adelaide, Australia: observations and a gravity wave-tidal interaction model. J. Atmos. Sci. 44 (3), 605–619.

Fritts, D.C., Wang, D., 1991. Doppler-shifting effects on frequency spectra of gravity waves observed near the summer mesopause at high latitude. J. Atmos. Sci. 48, 1535–1544.

Futyan, J.M., Del Genio, A.D., 2007. Deep convective system evolution over africa and the tropical atlantic. J. Clim. 20 (20), 5041–5060. https://doi.org/10.1175/JCLI4297.1.

Gavrilov, N.M., Manson, A.H., Meek, C.E., 1995. Climatological Monthly Characteristics of middle atmosphere Gravity waves (10min-10 h) during 1979-1993 at Saskatoon. AnnalesGeophysicae 13.285-295. https://doi.org/10.1007/s00585-995-0285-7.

Gavrilov, N.M., Riggin, D.M., Fritts, D.C., 2004. Interannual variations of the mean wind and gravity wave variances in the middle atmosphere over Hawaii. J. Atmos. Sol. Terr. Phys. 66 (6–9), 637–645. https://doi.org/10.1016/j.jastp.2004.01.015.

Gurubaran, S., Sridharan, S., Thokuluwa, R., Rajaram, R., 2001. The mesospheric quasi-2-day wave over Tirunelveli (8.7°N). J. Atmos. Sol. Terr. Phys. 63, 975–985. https://doi.org/10.1016/S1364-6826(01)00016-5.

Herman, R.L., Robinson, W.A., Franke, S.J., 1999. Observational evidence of quasi two-day/gravity wave interaction using MF Radar. Geophys. Res. Lett. 26 (8), 1141–1144. https://doi.org/10.1029/1999GL900157.

Hersbach, H., Bell, B., Berrisford, P., et al., 2020. The ERA5 global reanalysis. Q J R Meteorol. Soc. 146, 1999–2049. https://doi.org/10.1002/qj.3803.

Hines, C.O., 1960. Internal atmospheric gravity waves at ionospheric heights. Can. J. Phys. 38 (11), 1441–1481. https://doi.org/10.1139/p60-150.

Hodges, R.R., 1969. Eddy diffusion coefficients due to instabilities in internal gravity waves. J. Geophys. Res. 74 (16), 4087–4090. https://doi.org/10.1029/JA074i016p04087.

Holton, J.R., Beres, J.H., Zhou, X., 2002. On the vertical scale of gravity waves excited by localized thermal forcing. J. Atmos. Sci. 59 (12), 2019–2023. https://doi.org/10.1175/1520-0469(2002)059<2019:OTVSOG>2.0.CO;2.

Horinouchi, T., Nakamura, T., Kosaka, J.-I., 2002.Convectively generated mesoscale gravity waves simulated throughout the middle atmosphere. Geophys. Res. Lett., 29(21).https://doi.org/10.1029/2002GL016069

Isler, J. R., Fritts, D. C., 1996. Gravity Wave Variability and Interaction with Lower-Frequency Motions in the Mesosphere and Lower Thermosphere over Hawaii.Journal of Atmospheric Sciences. 53(1), 37-48.https://doi.org/10.1175/1520-0469(1996)053<0037:GWVAIW>2.0.CO;2

Jacobi, C., Gavrilov, N.M., Kürschner, D., Fröhlich, K., 2006. Gravity wave climatology and trends in the mesosphere/lower thermosphere region deduced from low-frequency drift measurements 1984–2003 (52.1°N, 13.2°E). J. Atmos. Sol. Terr. Phys. 68 (17), 1913–1923. https://doi.org/10.1016/j.jastp.2005.12.007.

Kawashima, M., 2003. The role of gravity waves in the meso-β-scale cycle of squall-line type convective systems. J. Meteor. Soc. Japan 81, 713–746. https://doi.org/10.2151/jmsj.81.713.

Kiladis, G.N., Dias, J., Straub, K.H., Wheeler, M.C., Tulich, S.N., Kikuchi, K., Weickmann, K.M., Ventrice, M.J., 2014. A comparison of OLR and circulation-based indices for tracking the MJO. Mon. Weather Rev. 142 (5), 1697–1715. https://doi.org/10.1175/MWR-D-13-00301.1.

Kovalam, S., Tsuda, T., Gurubaran, S., 2011. High-frequency gravity waves observed in the low-latitude mesosphere-lower thermosphere (MLT) region and their possible relationship to lower-atmospheric convection. J. Geophys. Res. 116, D15101. https://doi.org/10.1029/2011JD015625.

Kumar, K.K., 2006. VHF radar observations of convectively generated gravity waves: some new insights. Geophys. Res. Lett. 33, L01815. https://doi.org/10.1029/2005GL024109.

Liebmann, B., Smith, C.A., 1996. Description of a complete (interpolated) outgoing longwave radiation dataset. Bull. Am. Meteorol. Soc. 77, 1275–1277.

Lindzen, R.S., 1981. Turbulence and stress owing to gravity wave and tidal breakdown. J. Geophys. Res. Oceans 86 (C10), 9707–9714. https://doi.org/10.1029/JC086iC10p09707.

Liu, X., Yue, J., Xu, J., Garcia, R.R., Russell, J.M., Mlynczak, M., Wu, D.L., Nakamura, T., 2017. Variations of global gravity waves derived from 14 years of SABER temperature observations. J. Geophys. Res. 122, 6231–6249. https://doi.org/10.1002/2017JD026604.

Manson, A.H., Meek, C.E., Hall, G.E., 1998. Correlations of gravity waves and tides in the mesosphere over Saskatoon. J. Atmos. Sol. Terr. Phys. 60, 1089–1107. https://doi.org/10.1016/S1364-6826(98)00059-5.

Miyoshi, Y., Fujiwara, H., 2008. Gravity waves in the thermosphere simulated by a general circulation model. J. Geophys. Res. 113, D01101. https://doi.org/10.1029/2007JD008874.

Miyoshi, Y., Fujiwara, H., 2009. Gravity waves in the equatorial thermosphere and their relation to lower atmospheric variability. Earth Planet Sp. 61, 471–478. https://doi.org/10.1186/BF03353164.

Miyoshi, Y., Fujiwara, H., Jin, H., Shinagawa, H., 2014. A global view of gravity waves in the thermosphere simulated by a general circulation model. J. Geophys. Res.: Space Phys. 119, 5807–5820. https://doi.org/10.1002/2014JA019848.

Mlynczak, M.G., 1997. Energetics of the mesosphere and lower thermosphere and the SABER experiment. Adv. Space Res. 20 (6), 1177–1183. https://doi.org/10.1016/S0273-1177(97)00769-2.

Nakamura, T., Tsuda, T., Fukao, S., Manson, A.H., Meek, C.E., Vincent, R.A., Reid, I.M., 1996. Mesospheric gravity waves at Saskatoon (52° N), Kyoto (35°N) and Adelaide (35°S). J. Geophys. Res. 101 (D3), 7005–7012. https://doi.org/10.1029/95JD03826.

Narayanan, V.L., Gurubaran, S., 2013. Statistical characteristics of high frequency gravity waves observed by OH airglow imaging from Tirunelveli (8.7°N). J. Atmos. Sol. Terr. Phys. 92, 43–50. https://doi.org/10.1016/j.jastp.2012.09.002.

Narayanan, V.L., Gurubaran, S., Emperumal, K., 2010. Airglow imaging observations of small-scale structures driven by convective instability in the upper mesosphere over Tirunelveli (8.7°N). J. Geophys. Res. 115, D19119. https://doi.org/10.1029/2009JD012937.

Niranjan Kumar, K., Ramkumar, T., Krishnaiah, M., 2011. MST radar observation of inertia-gravity waves generated from tropical cyclones. J. Atmos. Sol. Terr. Phys. 73 (13), 1890–1906. https://doi.org/10.1016/j.jastp.2011.04.026.

Reid, I.M., Vincent, R.A., 1987. Measurements of the horizontal scales and phase velocities of short period mesospheric gravity waves at Adelaide, Australia. J. Atmos. Terr. Phys. 49 (10), 1033–1048. https://doi.org/10.1016/0021-9169(87)90110-3.

Sarkhel, S., Sekar, R., Chakrabarty, D., Guharay, A., 2012. Investigation on mesospheric gravity waves over Indian low latitude stations using sodium airglow observations and a few case studies based on thermal and wind structures. J. Atmos. Sol. Terr. Phys. 86, 41–50. https://doi.org/10.1016/j.jastp.2012.06.008.

Senft, D.C., Gardner, C.S., 1991. Seasonal variability of gravity wave activity and spectra in the mesopause region at Urbana. J. Geophys. Res. 96 (D9), 17229–17264. https://doi.org/10.1029/91JD01662.

Sonmor, L. J., Klaassen, G. P., 1997. Toward a Unified Theory of Gravity Wave Stability. Journal of the Atmospheric Sciences. 54(22), 2655-2680.https://doi.org/10.1175/1520-0469(1997)054<2655:TAUTOG>2.0.CO;2.

Sridharan, S., Sathishkumar, S., 2008. Seasonal and interannual variations of gravity wave activity in the low-latitude mesosphere and lower thermosphere over Tirunelveli (8.7° N, 77.8° E). Ann. Geophys. 26, 3215–3223. https://doi.org/10.5194/angeo-26-3215-2008.

Tian, C., Hu, X., Liu, Y., Cheng, X., Yan, Z., Cai, B., 2020. Seasonal Variations of High-Frequency Gravity Wave Momentum Fluxes and Their Forcing toward Zonal Winds in the Mesosphere and Lower Thermosphere over Langfang, China (39.4° N, 116.7° E).Atmosphere.11(11),1253. https://doi.org/10.3390/atmos11111253 .

Tsuda, T., Murayama, Y., Yamamoto, M., Kato, S., Fukao, S., 1990. Seasonal variation of momentum flux in the mesosphere observed with the MU radar. Geophys. Res. Lett. 17 (6), 725–728. https://doi.org/10.1029/GL017i006p00725.

Vadas, S.L., Fritts, D.C., 2004. Thermospheric responses to gravity waves arising from mesoscale convective complexes. J. Atmos. Sol. Terr. Phys. 66 (6–9), 781–804. https://doi.org/10.1016/j.jastp.2004.01.025.

Vadas, S.L., Yue, J., She, C.-Y., Stamus, P.A., Liu, A.Z., 2009. A model study of the effects of winds on concentric rings of gravity waves from a convective plume near Fort Collins on 11 May 2004. J. Geophys. Res. 114, D06103. https://doi.org/10.1029/2008JD010753.

Venkateswara Rao, N., Tsuda, T., Kawatani, Y., 2012. A remarkable correlation between short period gravity waves and semiannual oscillation of the zonal wind in the equatorial mesopause region. Ann. Geophys. 30, 703–710. https://doi.org/10.5194/angeo-30-703-2012.

Vincent, R.A., Fritts, D.C., 1987. A Climatology of Gravity Wave Motions in the Mesopause Region at Adelaide, Australia. Journal of the Atmospheric Sciences.44 (4), 748-760.https://doi.org/10.1175/1520-0469(1987)044<0748:ACOGWM>2.0.CO;2.

Vincent, R.A., Lesicar, D., 1991. Dynamics of the equatorial mesosphere: first results with a new generation partial reflection radar. Geophys. Res. Lett. 18 (5), 825–828. https://doi.org/10.1029/91GL00768.

Walterscheid, R.L., Christensen, A.B., 2016. Low-latitude gravity wave variances in the mesosphere and lower thermosphere derived from SABER temperature observation and compared with model simulation of waves generated by deep tropical convection. J. Geophys. Res. Atmos. 121, 11900–11912. https://doi.org/10.1002/2016JD024843.

Yiğit, E., Aylward, A.D., Medvedev, A.S., 2008. Parameterization of the effects of vertically propagating gravity waves for thermosphere general circulation models: sensitivity study. J. Geophys. Res. Atmos. 113, D19106. https://doi.org/10.1029/2008JD010135.

Yiğit, E., Medvedev, A.S., 2010. Internal gravity waves in the thermosphere during low and high solar activity: simulation study. J. Geophys. Res.: Space Phys. 115, A00G02. https://doi.org/10.1029/2009JA015106.

Yue, J., Hoffmann, L., Joan Alexander, M., 2013. Simultaneous observations of convective gravity waves from a ground-based airglow imager and the AIRS satellite experiment. J. Geophys. Res. Atmos. 118, 3178–3191. https://doi.org/10.1002/jgrd.50341.

Yue, J., Miller, S.D., Hoffmann, L., Straka III, W.C., 2014. Stratospheric and mesospheric concentric gravity waves over tropical cyclone Mahasen: joint AIRS and VIIRS satellite observations. J. Atmos. Sol. Terr. Phys. 119, 83–90. https://doi.org/10.1016/j.jastp.2014.07.003.

Zhang, K., Randel, W., Fu, R., 2017. Relationships between outgoing longwave radiation and diabatic heating in reanalyses. Clim. Dyn. 49. https://doi.org/10.1007/s00382-016-3501-0.